arXiv:1110.5751v1 [cond-mat.supr-con] 26 Oct 2011

Correlation enhanced electron-phonon coupling and high temperature superconductivity

Z. P. Yin[1,2],* A. Kutepov[1], and G. Kotliar[1]
[1]*Department of Physics and Astronomy, Rutgers University, Piscataway, New Jersey 08854, United States. and*
[2]*Department of Physics and Astronomy, Stony Brook University, Stony Brook, New York 11794, United States.*

(Dated: October 27, 2011)

The microscopic origin of superconductivity has been established in numerous classes of materials. In elemental metals it results from the exchange of phonons whereas in copper oxides and iron pnictides it is intimately connected to magnetism. On the other hand, the cause of superconductivity in $Ba_{1-x}K_xBiO_3$ (T_c =32 K)[1] and a large third class of isotropic high temperature superconductors is still mysterious and subject of debate.[2] Proposed mechanisms in bismuthates involve either the tendency of the Bi atoms avoiding the Bi^{4+} state, while preferring the Bi^{3+} and Bi^{5+} charge state thus generating an attractive local "negative U" pairing center[3, 4], or strong coupling to an O-breathing phonon mode[5, 6]. However, first principles calculations have so far ruled out both the negative U mechanism[7, 8] and the electron-phonon mechanism[9]. Here we demonstrate that dynamical correlations among electrons enhance their coupling to phonons in a large number of superconductors, raising significantly the previously underestimated theoretical superconducting critical temperature T_c of up to a few Kelvin to their experimental values of tens of Kelvin. The mechanism we propose is quite general, explains the magnitude and the doping dependence of superconductivity in many materials such as the celebrated $Ba_{1-x}K_xBiO_3$ compounds and the electron-doped β-HfNCl compounds (T_c = 25.5 K)10 and can be used to design other high temperature superconductors which have not yet been synthesized. As an application, we suggest $Ba_{1-x}La_xPbO_3$ with x ∼0.7 will superconduct above 10 K.

Earlier approaches to the electron phonon coupling (EPC) were based on the density functional theory (DFT) and linear response theory[11] in the local density approximation (LDA) or generalized gradient approximation (GGA). This approach correctly accounts for the rather high temperature superconductivity in elemental lithium (T_c ∼20 K)[12], yttrium (T_c ∼20 K)[13], calcium (T_c ∼25 K)[14] and binary compound MgB_2 (T_c ∼40 K)[15], so the results in ref [9] of rather small EPC strength $\lambda \simeq 0.3$ and very low T_c (up to 5 K) apparently rule out the phonon mechanism in $Ba_{1-x}K_xBiO_3$.

The widely used LDA/GGA exchange-correlation (EXC) functional in the DFT methodology, however, can suffer from large systematic errors in certain materials. These errors have been traced to two sources: failure to capture dynamic correlations because of self interaction errors or equivalently in the chemical sense failure to capture the delocalization of electrons due to Coulomb interaction (so-called delocalization errors in ref. [16]), and failure to capture static correlation effects resulting from degeneracies.[16] Treating static correlation effects requires multi-determinant methods such as DFT combined with dynamic mean field theory, whereas the dynamic correlations can be treated by using more sophisticated functionals such as hybrid functionals (HSE)[17] with nonlocal exchange potential. It has been recently pointed out[18, 19] that many difficulties in accounting for the physical properties of the $BaBiO_3$ related materials within standard DFT method, are due to dynamic correlations, and can be remedied by using hybrid functionals[17] or GW calculations which largely remove the LDA/GGA self interaction (dynamic correlation) effects. These improvements have resulted in excellent agreement with experiment for many computed physical properties, including crystal structure, lattice vibrations and optical conductivity.[18, 19]

Here we build on the insights of these works[18, 19] to address the problem of the superconducting mechanism in these materials. Using DFT and linear response theory[11] with both the conventional LDA/GGA functional and the non-local hybrid functional (HSE06)[17],(see supplementary material for calculational details) we evaluate the EPC, and find that the conventional functionals underestimates the EPC and predict the wrong trend with doping. On the other hand we find that once dynamic electronic correlations are taken into account, the EPC is sufficiently strong to account for the high temperature superconductivity in these materials.

The middle atom M in $BaBiO_3$ (BBO) and $BaPbO_3$ (BPO) is octahedrally coordinated by 6 oxygen atoms as in cuprate superconductors. Ideally without any distortion (eg. when optimal doped such as $Ba_{0.6}K_{0.4}BiO_3$), they crystallize in the simple cubic structure as shown in Fig. 1. However, the octahedral formed by oxygen atoms deviates from the ideal octahedral in the parent compounds.[20, 21] There are two types of distortions: one is the oxygen breathing distortion along nearest-

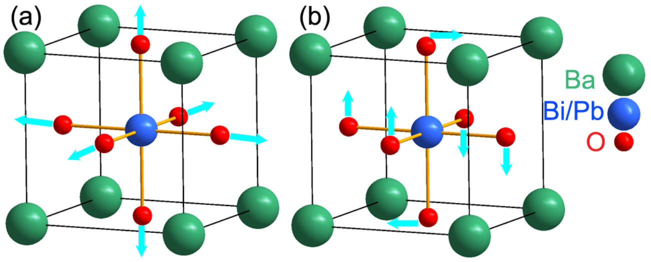

FIG. 1: **The crystal structure of BaBiO$_3$ and BaPbO$_3$.** (a)The oxygen breathing mode/distortion. (b)The oxygen tilting mode/distortion. Both oxygen breathing and tilting distortions exist in BaBiO$_3$ compound whereas only oxygen tilting distortion exists in BaPbO$_3$ compound.

neighbor M-O bonds as shown in Fig. 1(a). The other one is the oxygen tilting distortion perpendicular to the nearest-neighbor M-O bonds as shown in Fig. 1(b). Experimentally, both distortions exist in BBO whereas only O-tilting distortion exists in BPO.

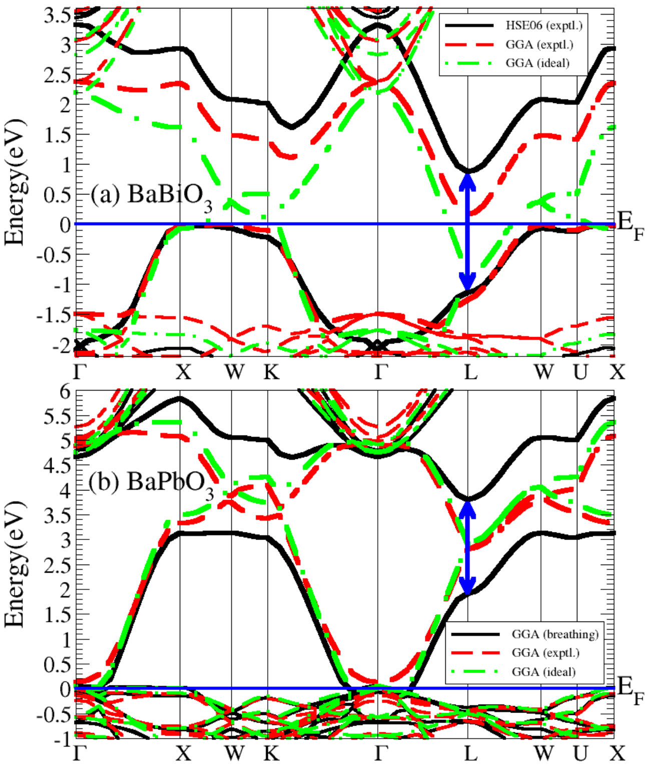

FIG. 2: **Band structure of BaBiO$_3$ and BaPbO$_3$.** The band structure of (a) BaBiO$_3$ and (b) BaPbO$_3$ calculated using both the GGA and HSE06 hybrid functionals with the ideal undistorted simple cubic structure, the experimental structure, and for BaPbO$_3$ an O-breathing distorted structure with O displacement of 0.085 $\AA$. Both GGA and HSE06 produce similar band structure at the ideal structure around the Fermi level. For BaPbO$_3$, the difference between GGA and HSE06 is less significant thus only GGA result is shown.

The deformation potential $D = \Delta\varepsilon_k/\Delta Q$ is an inexpensive way to measure the EPC strength, where ε_k is the band eigenvalue at k point and Q is the vibration amplitude. Large deformation potential is an indication of possible strong EPC. One example is provided by MgB$_2$. In first principle calculations, the deformation potential, however, depends on the EXC functional, signaling the crucial role of EXC functional in evaluating the EPC strength in real materials.

To demonstrate the EXC functional and M-atom dependence of the deformation potential, we show in Fig.2(a) the band structure of BaBiO$_3$ and BaPbO$_3$ with experimental and ideal structures using both GGA and HSE06 functionals in the folded face-centered cubic Brillouin zone. The deformation potential of BaBiO$_3$ from HSE06 functional of the conduction band (mostly of Bi $6s$ and O $2p$ states) across the Fermi level around L point, where the O-breathing instability occurs, is about 13.3 eV/$\AA$, which is almost twice of the GGA value 7.6 eV/$\AA$, and is even larger than the big deformation potential 13 eV/$\AA$ of the B E_{2g} breathing vibration mode found in the 40 K superconducting MgB$_2$ compound.[22] In BaPbO$_3$ compound, however, the same deformation potential given by GGA and HSE06 bears smaller difference, with values of 10.1 and 11.2 eV/$\AA$, respectively. The GGA deformation potential depends more strongly than HSE06 on the atom bonding to oxygen, specifically, the number of electrons of its outer shell. Using the virtual crystal approximation, we find that changing the charge of the M atom, the GGA deformation potential increases roughly linearly from M=Bi to Pb, whereas changing the charge of Ba atom barely changes the deformation potential.

The mode EPC strength λ_v can be estimated through the deformation potential, following ref.[22]

$$\lambda_v = N(\varepsilon_F)\frac{\hbar}{2M_O\omega_v^2}\sum_{j=1,2,3}|\hat{\varepsilon}_j\cdot\vec{D}_j|^2 \approx 1.4 \qquad (1)$$

for HSE calculations of the O-breathing mode in BaBiO$_3$, where the sum on j runs over the three moving O atoms of the O-breathing mode whose vibration frequency is ω_v ≈65 meV, and $N(\varepsilon_F)$=0.36 eV/states is the density of states per spin at the Fermi level contributed by the corresponding band whose average deformation potential on the Fermi surface is $\vec{D}_j$.

Alternatively, we can estimate the EPC strength by comparing the deformation potential of HSE with GGA/LDA functional coupled with the λ calculated from linear response calculations using GGA/LDA functional. Such an estimation is based on the fact that, the mode dependent EPC strength is proportional to squared deformation potential, i.e., $\lambda_v \propto D^2$, and the total λ is usually contributed mostly by only a few phonon modes.

We therefore has a simple relation of

$$\lambda_{HSE} \simeq |\frac{D_{HSE}}{D_{LDA/GGA}}|^2 * \lambda_{LDA/GGA}. \qquad (2)$$

The superconductivity in doped $BaBiO_3$ is mainly contributed by the O-breathing mode, analogous to the case of MgB_2 where the superconductivity is mainly driven by the B-breathing vibrations.[22]. The estimated $\lambda_{HSE} \approx 1.01$ based on the above deformation potentials and $\lambda_{LDA} = 0.33$ estimated from linear-response calculation, which is in agreement with previous LDA linear response calculations.[9] Using the modified McMillan equation

$$T_c = \frac{\omega_{log}}{1.20} exp(-\frac{1.04(1+\lambda)}{\lambda - \mu^*(1+0.62\lambda)}) \qquad (3)$$

with experimental average frequency $\omega_{log} \simeq 450$ K[23] and $\lambda \simeq 1.01$, T_c is estimated to be 31.8 K with μ^*=0.1 which is obtained by our first principle calculations (see supplementary material). As a result, the strong EPC strength $\lambda \simeq 1.0$ is enough to explain the rather high superconducting temperature $T_c \simeq 32$ K in K-doped $BaBiO_3$ in the framework of the conventional phonon mediated superconductivity.

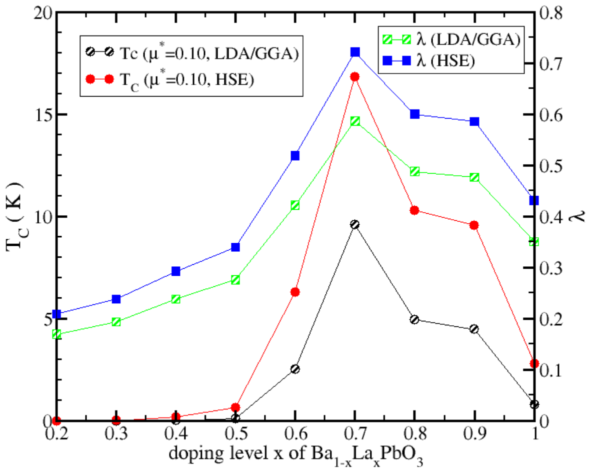

FIG. 3: **Electron-phonon coupling strength λ and superconducting T_c of $Ba_{1-x}La_xPbO_3$.** The doping effect is based on virtual crystal approximation. λ(LDA/GGA) is calculated from linear response and λ(HSE) is inferred from λ(LDA/GGA) according to equation (2).

Equation (2) can be further generalized to two isostructural compounds. As shown in Table I, the relation $\lambda^{BPO}_{LDA/GGA} \simeq (\frac{D^{BPO}_{LDA/GGA}}{D^{BBO}_{LDA/GGA}})^2 * \lambda^{BBO}_{LDA/GGA}$ holds for the optimal doped isostructural $BaBiO_3$ and $BaPbO_3$.

According to equation (2), the optimal λ_{HSE} for electron-doped $BaPbO_3$ is estimated to be 0.72, resulting in a superconducting T_c=16.7 K, assuming ω_{log}=450 K and μ^*=0.1. Therefore, superconductivity (T_c up to 16.7 K) is expected in electron-doped $BaPbO_3$ compounds. This is already confirmed experimentally by doping Bi/Sb into the Pb site, resulting in $T_c \sim 12$ K for $BaPb_{0.75}Bi_{0.25}O_3$ [24] and 3.5 K for $BaPb_{0.75}Sb_{0.25}O_3$ compound[25]. Here we show in Fig.3 that superconductivity may also be induced by doping into Ba site via studying the doping dependence of λ in $Ba_{1-x}La_xPbO_3$ based on virtual crystal approximation. The strong doping dependent λ suggests it is crucial to bring the Fermi level close to the bands with large deformation potential in order to optimize superconducting T_c.

The mechanism of dynamical correlation (particularly in $BaBiO_3$ nonlocal exchange) enhanced phonon mediated superconductivity seems very relevant to many materials where the electron bonding has both partially covalent (or metallic) and partially ionic character. There are precisely the materials where high temperature superconductors have been found. Our observation of enhanced EPC gives new insights into numerous mysteries.

In heavy fermion and copper oxide based materials, two dimensionality enhances superconductivity[26] but in $BaBiO_3$ related materials, layering by synthesis of $Ba_{n+1}Bi_nO_{3n+1}$ (n=1, 2, 3, $\cdots$) degrades the critical temperature instead. We have evaluated the deformation potential associated with O-breathing distortion and found it to be almost zero for the $Ba_3Bi_2O_7$ compound (n=2 member), resulting in very weak EPC and non-superconductivity, as seen in experiments[27]. For the Ba_2BiO_4 compounds (n=1 member), the corresponding deformation potential is about 70% of that in $BaBiO_3$. Optimal doped Ba_2BiO_4 compounds could be superconducting around 8 K, however, it hasn't been synthesized successfully in this form.

The mechanism described in this letter, has a broad range of applicability. Relatively high temperature superconductivity was discovered in electron doped MNX (M=Ti, Zr, and Hf; N=nitrogen; X=Cl, Br, and I). T_c is 16.5, 16 and 25.5 K for electron-doped α-TiNCl, β-ZrNCl and β-HfNCl, respectively. [28, 29] .

Also here, linear response calculation based on LDA functional produced λ about 0.52 and ω_{log} about 36.4 meV,[30] which gives T_c only 6 K assuming μ^*=0.1 and is insufficient to account for its 16 K superconductivity, raising the question of what is the mechanism of superconductivity. A proper theory should explain why β-HfNCl has higher T_c than β-ZrNCl and why T_c in these electron-doped MNX compounds depends weakly on the doping level and the X atom. In other known high temperature superconductors, including the BaBiO3 based ones, the critical temperature depends crucially on the level of doping. Our calculations indicate that in the electron-doped β-ZrNCl compound, the deformation potential of the conduction bands (see supplementary material) associated with Zr-N vibration along c direction is substantially enhanced from 4.0 eV/$\AA$ in GGA to 4.7 eV/$\AA$ in HSE functional. The enhanced deformation potential results in $\lambda \sim 0.72$ and T_c=15.7 K (assuming ω_{log}=36.4 meV and μ^*=0.1), in close agreement with ex-

TABLE I: **Various quantities for selected compounds.** Deformation potential D (eV/$\AA$) from GGA and HSE functionals for the most important vibration mode, electron-phonon coupling constant λ from linear response calculations (LDA/GGA) and inferred value for HSE according to equation (2), average phonon frequency ω_{log} (K) from linear response calculations (LDA/GGA) and experiments, the calculated optimal superconducting temperature T$_c$ (K) by LDA/GGA and HSE functionals (assuming μ^*=0.10) and experimental T$_c$ for selected compounds with proper electron or hole doping.

Compounds	mode	D (GGA)	D (HSE)	λ(LDA/GGA)	λ (HSE)	ω_{log}	T$_c$(LDA/GGA)	T$_c$ (HSE)	T$_c$ (exp.)
$BaBiO_3$	O-Bi-O	7.6	13.3	0.33	1.01	450	0.5	31.8	32.0 [1]
$BaPbO_3$	O-Pb-O	10.1	11.2	0.58	0.72	450	9.3	16.7	12.0 [24]
$Ba_3Bi_2O_7$	O-Bi-O	∼0	∼0	∼0	∼0	∼450	∼0	∼0	<2 [27]
ZrNCl	Zr-N	4.0	4.7	0.52	0.72	422	6.0	15.7	16 [29]
HfNCl	Hf-N	4.4	5.3		0.91	422	–	25.2	25.5 [10]
TiNCl	Ti-N	3.8	4.6		0.70	422	–	14.7	16.5 [28]

perimental value of 16.0 K. More importantly, the same deformation potential is substantially larger in β-HfNCl than in β-ZrNCl, which is increased from 4.4 eV/$\AA$ in GGA to 5.3 eV/$\AA$ in HSE. Since β-HfNCl is isostructural to β-ZrNCl, the 5.3 eV/$\AA$ deformation potential gives $\lambda \sim 0.91$ and T$_c$=25.2 K for electron-doped β-HfNCl, in good agreement with experiment. It explains naturally the higher T$_c$ in β-HfNCl than β-ZrNCl. The 16.5 K superconductivity in electron-doped α-TiNCl can also be well accounted for in the same way as shown in Table I. Therefore linear response calculations with hybrid functional can fully account for the observed superconducting T$_c$ in these electron-doped MNX compounds. We expect that the unexpected high T$_c$ superconductivity in many other superconductors including those reviewed in ref.[31] can be explained in a similar way by incorporating appropriate EXC functional.

As a final remark, we stress that first principle calculations based on LDA/GGA functional can significantly underestimate the EPC strength due to the failure to capture dynamic correlations. As a result, critical reexamination of the role of EPC in many superconductors including cuprate superconductors and recently discovered iron-based superconductors is called for by applying appropriate EXC functional such as HSE. The superconductivity in many exotic superconductors therefore could be reconciled with phonon-mediated mechanism. Our study demonstrate that deformation potential can serve as a fast and effective criteria for searching potential phonon-mediated high T$_c$ superconductors and doping is crucial to optimize T$_c$ in this class of systems.

---

[*] Electronic address: yinzping@physics.rutgers.edu

[1] Cava, R. J. *et al.* Superconductivity near 30 K without copper: the $Ba_{0.6}K_{0.4}BiO_3$ perovskite. *Nature* **332**, 814-816 (1988).

[2] Pickett, W. E. The other high-temperature superconductors. *Physica B* **296**, 112-119 (2001).

[3] Taraphder, A., Krishnamurthy, H. R., Pandit, R. & Ramakrishnan, T. V. Negative-U extended Hubbard model for doped barium bismuthates. *Phys. Rev. B* **52**, 1368-1388 (1995).

[4] Varma, C. M. Missing valence states, diamagnetic insulators, and superconductors. *Phys. Rev. Lett.* **61**, 2713-2716 (1988).

[5] Jin, W., Degani, M. H., Kalia, R. K. & Vashishta, P. Superconductivity in $Ba_{1-x}K_xBiO_3$. *Phys. Rev. B* **45**, 5535-5546 (1992).

[6] Rice, T. M. & Sneddon, L. Real-space and $\vec{k}$-space electron pairing in $BaPb1_{1-x}Bi_xO_3$. *Phys. Rev. Lett.* **47**, 689-692 (1981).

[7] Vielsack, G. & Weber, W. Search for negative U in the $Ba_{1-x}K_xBi_{1-y}Pb_yO_3$ system using constrained density-functional theory. *Phys. Rev. B* **54**, 6614-6623 (1996).

[8] Harrison, W. A. Valence-skipping compounds as positive-U electronic systems. *Phys. Rev. B* **74**, 245128 (2006).

[9] Meregalli, V. & Savrasov, S. Y. Electron-phonon coupling and properties of doped $BaBiO_3$. *Phys. Rev. B* **57**, 14453-14469 (1998).

[10] Yamanaka, S., Hotehama, K.-I. & Kawaji, H. Superconductivity at 25.5 K in electron-doped layered hafnium nitride. *Nature* **392**, 580-582 (1998).

[11] Savrasov, S. Y. Linear-response theory and lattice dynamics: a muffin-tin-orbital approach. *Phys. Rev. B* **54**, 16470-16486 (1996).

[12] Kasinathan, D. *et al.* Superconductivity and lattice instability in compressed lithium from Fermi surface hot spots. *Phys. Rev. Lett.* **96**, 047004 (2006).

[13] Yin, Z. P., Savrasov, S. Y. & Pickett, W. E. Linear response study of strong electron-phonon coupling in yttrium under pressure. *Phys. Rev. B* **74**, 094519 (2006).

[14] Yin, Z. P., Gygi, F. & Pickett, W. E. Competing phases, strong electron-phonon interaction, and superconductivity in elemental calcium under high pressure. *Phys. Rev. B* **80**, 184515 (2009).

[15] Kong, Y., Dolgov, O. V., Jepsen, O. & Andersen, O. K. Electron-phonon interaction in the normal and superconducting states of MgB_2. *Phys. Rev. B* **64**, 020501(R) (2001).

[16] Cohen, A. J., Mori-Sánchez, P. & Yang, W. T. Insights into current limitations of density functional theory. *Science* **321**, 792-794 (2008).

[17] Krukau, A. V., Vydrov, O. A., Izmaylov, A. F. & Scuseria, G. E. Influence of the exchange screening parameter on the performance of screened hybrid functionals. *J. Chem. Phys.* **125**, 224106 (2006).

[18] Franchini, C., Kresse, G. & Podloucky, R. Polaronic Hole Trapping in Doped $BaBiO_3$. *Phys. Rev. Lett.* **102**, 256402 (2009).

[19] Franchini, C., Sanna, A., Marsman, M. & Kresse, G. Structural, vibrational, and quasiparticle properties of the Peierls semiconductor $BaBiO_3$: a hybrid functional and self-consistent GW+vertex-corrections study. *Phys. Rev. B* **81**, 085213 (2010).

[20] Cox, D. E. & Sleight, A. W. Mixed-valent $Ba_2Bi^{3+}Bi^{5+}O_6$: structure and properties *vs* temperature. *Acta Cryst.* **B35**, 1-10 (1979).

[21] Fu, W. T., Visser, D. & IJdo, D. J. W. High-resolution neutron powder diffraction study on the structure of $BaPbO_3$. *Solid State Commun.* **134**, 647-652 (2007).

[22] An, J. M. & Pickett, W. E. Superconductivity of MgB_2: covalent bonds driven metallic. *Phys. Rev. Lett.* **86**, 4366-4369 (2001).

[23] Loong, C.-K. *et al.* Phonon density of states and oxygen-isotope effect in $Ba_{1-x}K_xBiO_3$. *Phys. Rev. B* **45**, 8052-8064 (1992).

[24] Sleight, A. W., Gillson, J. L. & Bierstedt, P. E. High-temperature superconductivity in the $BaPb_{1-x}Bi_xO_3$ systems. *Solid State Commun.* **17**, 27-28 (1975).

[25] Cava, R. J. *et al.* Superconductivity at 3.5 K in $BaPb_{0.75}Sb_{0.25}O_3$: why is T_c so low? *Nature* **339**, 291-293 (1989).

[26] Monthoux, P.& Lonzarich, G. G. Magnetically mediated superconductivity:crossover from cubic to tetragonal lattice. *Phys. Rev. B* **66**, 224504 (2002).

[27] Cava, R. J. *et al.* $(Ba,K)_3Bi_2O_7$: a layered bismuth oxide. *Phys. Rev. B* **44**, 9746-9748 (1991).

[28] Yamanaka, S., Yasunaga, T., Yamaguchi, K. & Tagawa, M. Structure and superconductivity of the intercalation compounds of TiNCl with pyridine and alkali metals as intercalants. *J. Mater. Chem.* **19**, 2573-2582 (2009).

[29] Yamanaka, S. High-T_c superconductivity in electron-doped layer structured nitrides. *Annu. Rev. Mater. Sci.* **30**, 53-82 (2000).

[30] Heid, R. & Bohnen, K.-P. *Ab initio* lattice dynamics and electron-phonon coupling in Li_xZrNCl. *Phys. Rev. B* **72**, 134527 (2005).

[31] Pickett, W. E. The next breakthrough in phonon-mediated superconductivity. *Physica C* **468**, 126-135 (2008).

Supplementary Information is linked to the online version of the paper at www.nature.com.

Author Information: Correspondence and requests for materials should be addressed to ZPY at yinzping@physics.rutgers.edu.

Acknowledgments We are grateful to Mac Beasley and Bob Cava for interesting us in this problem. ZPY and GK were supported by the AFOSR. This research was supported in part by the National Science Foundation through TeraGrid resources provided by Ranger (TACC) under grant number TG-DMR100048.

Author Contributions: This project was led by ZPY who carried out the large majority of the calculations, their analysis and their interpretation. AK developed and carried out the calculations of μ^* and U. ZPY and GK conceived the project and wrote the manuscript. All authors have read and commented on the manuscript.

Correlation enhanced electron-phonon coupling and high temperature superconductivity: Supplementary online material

Z. P. Yin[1,2], A. Kutepov[1], and G. Kotliar[1]
[1]*Department of Physics and Astronomy, Rutgers University, Piscataway, New Jersey 08854, United States.*
[2]*Department of Physics and Astronomy, Stony Brook University, Stony Brook, New York 11794, United States.*

Method

The electronic structures are calculated using both the VASP[S1] code with GGA(PBE)[S2] and HSE06[S3] exchange-correlation functionals and WIEN2k[S4] code with GGA(PBE)[S2] exchange-correlation functional. Linear response calculations are carried out using the LMTART[S5, 6] code with the ideal cubic structures (i.e., without distortions). The crystal structures are taken from ref.S[7] for $BaBiO_3$ and ref. S[8] for $BaPbO_3$. For VASP calculations, the PAW-PBE pseudopotential is used, which is also coupled with the HSE calculations. The energy cutoff for the wavefunction is 400 eV. The results of GGA calculations from VASP are double checked with results from WIEN2k with GGA(PBE) exchange-correlation functional. In linear response calculations, a 32^3 k mesh is used to converge the electron charge density. The electron phonon coupling constant is obtained with a 8^3 q mesh with 35 independent q points in the irreducible Brillouin zone. We use virtual crystal approximation to simulate doping effect.

Evaluating Coulomb pseudopotential

To estimate the Coulomb pseudopotential μ^*, we implemented the methodology of Ref.[S9] in our codes[S10, 11] which combine LDA and GW methods in a linearized augmented plane-wave (LAPW) basis set. μ^* is given by the formula

$$\mu^* = \frac{\mu}{1+\mu \ln \frac{\varepsilon_F}{\omega_D}} \tag{4}$$

where ε_F is the Fermi energy and ω_D the Debye energy, and dimensionless parameter μ is calculated as the following average over Fermi surface

$$\mu = N(E_F)\frac{\sum_{\mathbf{k}\mathbf{k}'}\sum_{\lambda\lambda'} W_{\mathbf{k}\lambda;\mathbf{k}'\lambda'}\delta(\varepsilon_{\mathbf{k}\lambda}-E_F)\delta(\varepsilon_{\mathbf{k}'\lambda'}-E_F)}{\sum_{\mathbf{k}\mathbf{k}'}\sum_{\lambda\lambda'}\delta(\varepsilon_{\mathbf{k}\lambda}-E_F)\delta(\varepsilon_{\mathbf{k}'\lambda'}-E_F)}, \tag{5}$$

where $N(E_F)$ is the density of states at Fermi level per spin, $\varepsilon_{\mathbf{k}\lambda}$ is the Kohn-Sham eigenvalue of the λth band at a wave vector $\mathbf{k}$, and matrix elements of the screened Coulomb interaction in a basis of LDA eigenstates are calculated as the following

$$W_{\mathbf{k}\lambda;\mathbf{k}'\lambda'} = \langle \mathbf{k}'\lambda' \uparrow, -\mathbf{k}'\lambda' \downarrow |W| \mathbf{k}\lambda \uparrow, -\mathbf{k}\lambda \downarrow\rangle. \tag{6}$$

The resulting μ^* for the ideal $BaBiO_3$, $BaPbO_3$ and $LaPbO_3$ compounds are 0.104, 0.117 and 0.119 respectively.

The difference between our work and Ref. S9 is that we use finite temperature formalism and approximate δ function with the imaginary part of LDA Matsubara's Green's function

$$\delta(\varepsilon_{\mathbf{k}\lambda}-E_F) \approx Im\frac{1}{i\omega_0+E_F-\varepsilon_{\mathbf{k}\lambda}}, \tag{7}$$

where ω_0 is the smallest positive Matsubara's frequency. The expression (7) becomes exact in the limit of zero temperature. Technically we perform the following steps. First we calculate LDA one-electron spectrum and corresponding wave functions. It provides us with LDA Green's function. Then we evaluate LDA polarizability $P_{LDA} = G_{LDA}G_{LDA}$. The third step is to calculate screened interaction $W = V + VP_{LDA}W$, where V is bare Coulomb interaction. After the third step we are able to get the Coulomb pseudopotential parameter.

Density of States

The HSE06 functional also describe the doped compounds better. We show in Fig.S1 the calculated density of states (DOS) of an optimal doped compound $Ba_{0.62}K_{0.38}BiO_3$ using both the PBE functional and HSE06 functional, based on virtual crystal and rigid band approximation, and we compare them with the experimental ultraviolet photoemission spectra[S12] (UPS) of $Ba_{0.62}K_{0.38}BiO_3$. We note that the rigid band approximation is as good as the virtual crystal approximation since we use the experimental structure. There is an overall good agreement between the DOS from HSE06 calculation and experimental UPS, in particular they share roughly the same peak centered at about -3.1 eV. In contrast, the DOS from PBE calculation has a peak centered at about -2.2 eV.

Optical conductivity

The optical conductivity offer a baseline to assess the electronic structure and importance of electronic correlations. We plot in Fig. S2 the optical conductivity for the parent $BaBiO_3$ and $BaPbO_3$ compounds (with distortions) and the optical conductivity and effective number

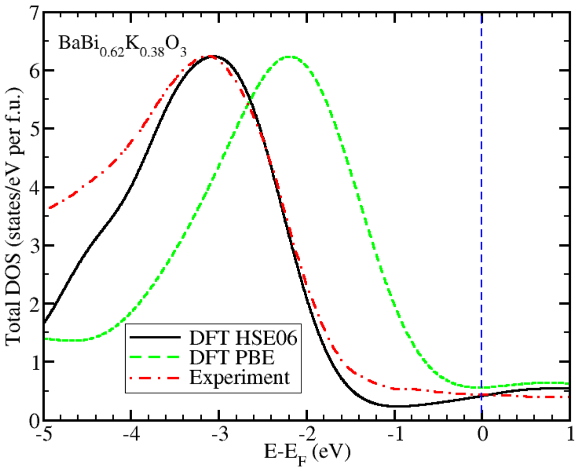

FIG. S1: **Density of states of Ba$_{0.62}$K$_{0.38}$BiO$_3$.** The DOS of Ba$_{0.62}$K$_{0.38}$BiO$_3$ calculated using both the PBE functional and HSE06 hybrid functional. The experimental data is the ultraviolet photoemission spectra taken from Ref. S12.

of charge carrier for the 0.38 K-doped Ba$_{0.62}$K$_{0.38}$BiO$_3$ compound in the cubic structure.

For the parent BaBiO$_3$ compound, the DFT-PBE peak position in the optics shows a clear deviation (0.5 eV) from the experimental value as shown in Fig. S2(a). The HSE06 functional over-corrects the DFT-PBE peak position, resulting in an overestimation of 0.3 eV. The best match is obtained by confining the non-local Fock exchange within certain distance through a control parameter μ=0.5, for which HSE functional is denoted as mHSE in Fig. S2. Note that $\mu = 0$ corresponds to no confinement of the Fock exchange, i.e., the PBE0 functional, $\mu = \infty$ corresponds to no Fock exchange is included, which restores to the PBE functional, while $\mu = 0.2$ lies between the two limits and corresponds to the HSE06 functional. Similarly, the HSE06 functional improves over DFT-PBE in the optics of BaPbO$_3$ compound as shown in Fig. S2(b).

For the Ba$_{0.62}$K$_{0.38}$BiO$_3$ compound, by comparing the experimental and DFT-PBE calculated optical conductivity and the energy-dependent effective number of charge carrier shown in Fig. S2(c) and (d), we estimate an overall mass enhancement of $m^*/m_{band} \sim 2$ in the low energy region, in consistent with the specific heat measurement of m^*/m_{band} up to 1.8.[S16] As discussed in the main article, the strong electron-phonon coupling ($\lambda \simeq$1.0) in the optimal doped BaBiO$_3$ gives rise to a mass enhancement of $m^*/m_{band} = 1 + \lambda \sim 2$ thus is able to account for the above mass enhancement. Therefore, the effect of static electronic correlation in BaBiO$_3$ is mild.

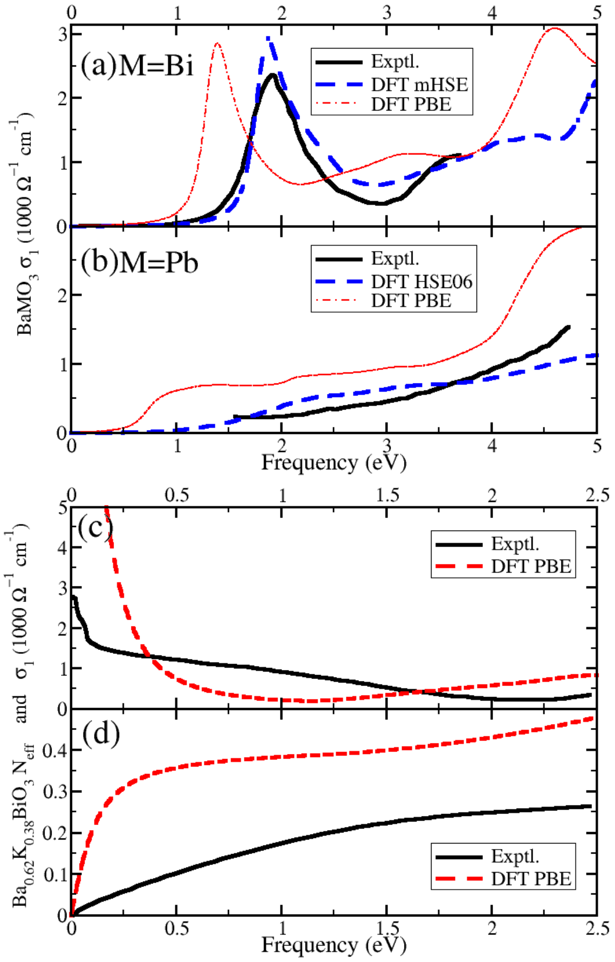

FIG. S2: **Optical conductivity and effective charge carrier number.** (a) and (b): the optical conductivity for the parent compound of BaBiO$_3$ and BaPbO$_3$, respectively. (c) the optical conductivity and (d) the resulting effective carrier number N$_{eff}$ for Ba$_{0.62}$K$_{0.38}$BiO$_3$. We compare the calculated results obtained by using both the PBE functional and HSE hybrid functional with available experimental data which are taken from Ref. S13–15

Lattice distortions and phonon softening

We compute the total energy as a function of the two main distortions, i.e., O-breathing and O-tilting distortions. The results are shown in figure S3 in the stoichiometric compounds. The inclusion of nonlocal exchange has a dramatical effect on the lattice dynamics in BaBiO$_3$ but less so in BaPbO$_3$. Compared to standard PBE calculations, the O-breathing instability is dramatically enhanced in the mHSE and HSE06 calculations in BaBiO$_3$ as suggested by the energy barrier[S17] (0.25 eV/f.u. in HSE06 *vs* almost 0 eV/f.u. in PBE) shown in Fig.S3 (a) and (b), whereas there is no O-breathing instability in BaPbO$_3$ in both PBE and HSE06 calculations as shown in Fig.S3 (d). For the tilting distortion on the other hand, the energy barriers ($\sim 0.1 eV/f.u.$,

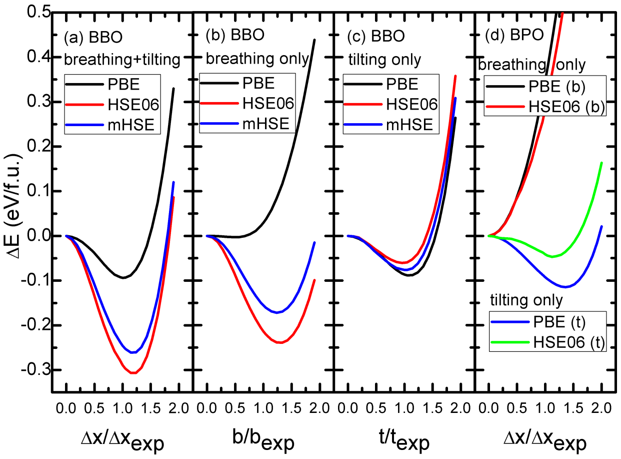

FIG. S3: **Total energy under distortions.** The change of the total energy as a function of O-breathing distortion and O-tilting distortion from its ideal positions obtained by PBE functional and HSE hybrid functional (HSE06 and mHSE) in DFT calculations for $BaBiO_3$ compound (a, b, c) and $BaPbO_3$ compound (d). The distortions are normalized to its experimental distortion, i.e., $\Delta x/\Delta x_{exp}$. Since experimentally there is no O-breathing distortion in $BaPbO_3$ compounds, its O-breathing distortion is normalized to the experimental distortion in $BaBiO_3$ compound.

FigS3 (c) and (d)) are substantially smaller than the energy barrier 0.25 eV/f.u. of O-breathing distortion in HSE calculations. Note the PBE calculations have slightly larger energy barrier than HSE calculations for the tilting distortion. These results suggest that for the $BaBiO_3$ compound, the HSE functional strongly softens the O-breathing phonon frequency compared to PBE functional. This is reflected in the average phonon frequency ω_{log}, which in the LDA calculation[S18] ω_{log} is about 550 K, while in experiments[S19, 20] which resemble the HSE functional calculation, is substantially smaller, only 450 K.

Band structure of β-HfNCl

The DFT-PBE band structure and density of states of β-HfNCl is shown in Fig.S4, which is calculated with its experimental crystal structure[S21] without/with Hf atom shifted along the *c*-axis to change the Hf-N bonding length. In the calculations, the experimental stacking of the layers along the *c*-axis is ignored for simplicity. As the arrows indicated in the left panel of Fig.S4, there is substantial deformation potential for the first two conduction bands, which are very flat along the Γ-Z symmetry line, resulting in a high density of states as shown in the right panel of Fig.S4. Such a high density of states makes electron-doping hardly change the chemical potential in this region. The flat bands with substantial deformation potential is therefore likely the reason that the T_c is weakly doping-dependent in electron-doped β-HfNCl compounds and other doped MNX compounds.

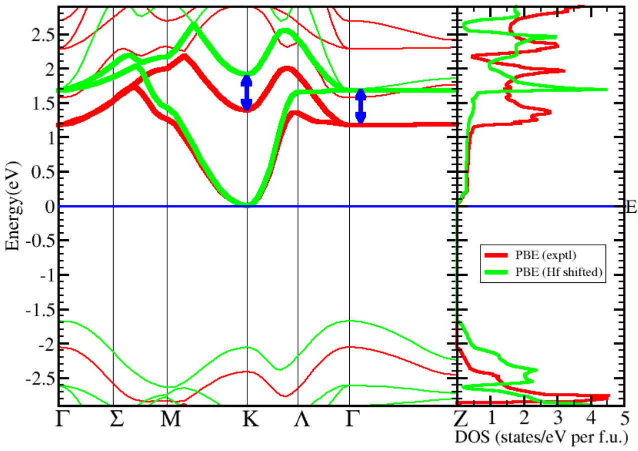

FIG. S4: **Band structure and density of states of β-HfNCl.** The band structure and density of states of β-HfNCl calculated using the PBE functional with the experimental crystal structure[S21] and with the experimental crystal structure except the Hf atom is shifted along the *c*-axis such that the Hf-N bond is shortened by 0.09 $\AA$. For simplicity, the different layer stacking along *c*-axis is ignored.

---

[*] Electronic address: yinzping@physics.rutgers.edu

[S1] Kresse, G. & Furthmüller, J. Efficiency of *ab-initio* total energy calculations for metals and semiconductors using a plane-wave basis set. *Comput. Mater. Sci.* **6**, 15-50 (1996).

[S2] Perdew, J. P., Burke, K. & Ernzerhof, M. Generalized gradient approximation made simple. *Phys. Rev. Lett.* **77**, 3865-3868 (1996).

[S3] Krukau, A. V., Vydrov, O. A., Izmaylov, A. F. & Scuseria, G. E. Influence of the exchange screening parameter on the performance of screened hybrid functionals. *J. Chem. Phys.* **125**, 224106 (2006).

[S4] Blaha, P., Schwarz, K., Madsen, G. K. H., Kvasnicka, D. & Luitz, J. WIEN2K An augmented plane wave + local orbitals program for calculating crystal properties, (K. Schwarz, Techn. Univ. Wien, Austria, 2001).

[S5] Savrasov, S. Y. Linear-response theory and lattice dynamics: a muffin-tin-orbital approach. *Phys. Rev. B* **54**, 16470-16486 (1996).

[S6] Savrasov, S. Y. & Savrasov, D. Y. Electron-phonon interactions and related physical properties of metals from linear-response theory. *Phys. Rev. B* **54**, 16487-16501 (1996).

[S7] Cox, D. E. & Sleight, A. W. Mixed-valent $Ba_2Bi^{3+}Bi^{5+}O_6$: structure and properties *vs* temperature. *Acta Cryst.* **B35**, 1-10 (1979).

[S8] Fu, W. T., Visser, D. & IJdo, D. J. W. High-resolution neutron powder diffraction study on the structure of $BaPbO_3$. *Solid State Commun.* **134**, 647-652 (2007).

[S9] Lee, K.-H., Chang, K. J. & Cohen, M. L. First-principles calculations of the Coulomb pseudopotential μ^*: application to Al. *Phys. Rev. B* **52**, 1425-1428 (1995).

[S10] Kutepov, A. L. & Kutepova, S. G. The *ab initio* ground state properties and magnetic structure of plutonium. *J. Phys.: Condens. Matter* **15**, 2607-2624 (2003).

[S11] Kutepov, A., Savrasov, S. Y. & G. Kotliar, G. Ground-state properties of simple elements from GW calculations. *Phys. Rev. B* **80**, 041103 (2009).

[S12] Namatame, H. *et al.* Effects of hole doping and electron-phonon interaction on the electronic structure of $\mathrm{Ba}_{1-x}\mathrm{K}_x\mathrm{BiO}_3$ studied by photoemission spectroscopy. *Phys. Rev. BS* **50**, 13674-13678 (1994).

[S13] Ahmad, J. & Uwe, H. Small-polaron excitations in $\mathrm{Ba}_{1-x}\mathrm{K}_x\mathrm{BiO}_3$ studied by optical reflectivity measurements. *Phys. Rev. B* **72**, 125103 (2005).

[S14] Puchkov, A. V. *et al.* Doping dependence of the optical properties of $\mathrm{Ba}_{1-x}\mathrm{K}_x\mathrm{BiO}_3$. *Phys. Rev. B* **54**, 6686-6692 (1996).

[S15] Wang, Y. Y., Feng, G. F., Sutto, T. E. & Han, P. D. Dielectric function of $\mathrm{BaPb}_{1-x}\mathrm{Bi}_x\mathrm{O}_3$ investigated by ellipsometry. *Phys. Rev. B* **48**, 16006-16010 (1993).

[S16] Graebner, J. E., Schneemeyer, L. F., & Thomas, J. K. Heat capacity of superconducting $\mathrm{Ba}_{0.6}\mathrm{K}_{0.4}\mathrm{BiO}_3$ near T_c. *Phys. Rev. B* **39**, 9682-9684 (1989).

[S17] The energy barrier is defined as the energy difference between the total energy without structural distortion and the minimal total energy with certain structural distortion.

[S18] Meregalli, V. & Savrasov, S. Y. Electron-phonon coupling and properties of doped BaBiO_3. *Phys. Rev. B* **57**, 14453-14469 (1998).

[S19] Loong, C.-K. *et al.* Phonon density of states and oxygen-isotope effect in $\mathrm{Ba}_{1-x}\mathrm{K}_x\mathrm{BiO}_3$. *Phys. Rev. B* **45**, 8052-8064 (1992).

[S20] Prassides, K., Rosseinsky, M. J., Dianoux, A. J. & Day, P. Temperature and composition evolution of the phonon density of states in $\mathrm{(Ba,K)(Pb,Bi,Sb)O}_3$ ceramic oxides. *J. Phys. Condens. Matter* **4**, 965-975 (1992).

[S21] Chen, X.-A., Koiwasaki, T. & Yamanaka, S. High-pressure synthesis and crystal structures of β-MNCl (M=Zr and Hf). *J. Solid State Chem.* **159**, 80-86 (2001).